Risk of climate-induced damage in historic textiles

Journal:	*Strain*
Manuscript ID:	Draft
Manuscript Type:	Full Paper
Date Submitted by the Author:	n/a
Complete List of Authors:	Bratasz, Łukasz; The National Museum in Krakow, ; Jerzy Haber Institute of Catalysis and Surface Chemistry Polish Academy of Sciences, Łukomski, Michał; Jerzy Haber Institute of Catalysis and Surface Chemistry Polish Academy of Sciences, Klisińska-Kopacz, Anna; The National Museum in Krakow, Zawadzki, Witold; Marian Smoluchowski Institute of Physics, Jagiellonian University, Dzierzega, Krzysztof; Marian Smoluchowski Institute of Physics, Jagiellonian University, Bartosik, Marcin; Marian Smoluchowski Institute of Physics, Jagiellonian University, Sobczyk, Joanna; The National Museum in Krakow, Lennard, Frances; Centre for Textile Conservation and Technical Art History, University of Glasgow, Kozłowski, Roman; Jerzy Haber Institute of Catalysis and Surface Chemistry Polish Academy of Sciences,
Keywords:	textiles, damage, climate, hygral expansion, tensile properties

Risk of climate-induced damage in historic textiles

Ł. Bratasz[1,2], M. Łukomski[2*], A. Klisińska-Kopacz[1], W. Zawadzki[3], K. Dzierżęga[3], M. Bartosik[3], J. Sobczyk[1], F. J. Lennard[4] and R. Kozłowski[2]

[1]The National Museum in Krakow, al. 3 Maja 1, 30-062 Kraków, Poland

[2]Jerzy Haber Institute of Catalysis and Surface Chemistry, Polish Academy of Sciences, ul. Niezapominajek 8, 30-239 Kraków, Poland

[3]Marian Smoluchowski Institute of Physics, Jagiellonian University, ul. Reymonta 4, 30-059 Kraków, Poland

[4]Centre for Textile Conservation and Technical Art History, University of Glasgow, Glasgow, G12 8QQ, UK

[*]the corresponding author: e-mail: nclukoms@cyf-kr.edu.pl, tel.: +48-12-6395152, fax: +48-12-4251923

Short running head title: Risk of damage in historic textiles

ABSTRACT: Eleven wool and silk historic textiles and two modern artist's canvases were examined to determine their water-vapour adsorption, moisture dimensional response and tensile behaviour. All the textiles showed a similar general pattern of moisture response. A rise in ambient relative humidity (RH) from dry conditions produced expansion of a textile until a certain critical RH level after which a contraction occurred to a greater or lesser degree depending on the yarn crimp and the weave geometry. The largest expansion recorded between the dry state and 80% RH was 1.2 and 0.9% for wool and silk textiles, respectively. The largest shrinkage of 0.8% at high RH range was experienced by a modern linen canvas. Two potential damage mechanisms related to the moisture response of the textiles - stress building due to shrinkage of the textile restrained in its dimensional response and the fretting fatigue when yarns move with friction one against another - were found insignificant in typical textile display environments unless the textiles are severely degraded or excessively strained in their mounting.

KEY WORDS: *textiles, damage, climate, hygral expansion, tensile properties*

Introduction [heading]

The biopolymer building-blocks of natural fibres, from which historic textiles were produced, are hygroscopic materials which gain moisture when the relative humidity (RH) is high, or lose moisture when the surrounding air is dry. A characteristic pattern of textile dimensional change, termed 'hygral expansion', is observed as a consequence of moisture adsorption by the fibres [1]. A rise in fibre moisture content (MC) from dry conditions produces expansion of a textile until a certain critical MC level (about 20% for wool), after which a contraction occurs. The initial expansion at relatively low MC levels is caused by fibre swelling forces and a reduction of weave crimp in the yarns (de-crimping) as the fibres straighten, increasing the yarn length and decreasing the number of waves per unit length. However as warp and weft yarns swell to a level of mutual constriction, the expansion of the textile ceases. The separation of the centres of the yarns at the cross-over points increases, leading to a reduction in the spacing between adjacent threads and overall shrinkage.

This pattern of textile hygral expansion was confirmed by several studies of fabric painting supports undertaken as part of a broader attempt to understand the physical behaviour of whole paintings [2-4]. 75-85% RH was established as the region at which shrinkage, sometimes dramatic, can be observed in linen fabrics. A 12 oz. cotton duck showed shrinkage even in the initial RH region on the step increase in RH from 10 to 40% [5]. When restrained during shrinkage, significant forces can develop in the textile. The effect was pronounced in tightly woven fabrics for yarns with high crimp but was not observed for straight yarns. Hedley further demonstrated that the fabrics can undergo a plastic re-configuration above 80% RH to compensate for the stresses [2]. The structural rearrangement may proceed stepwise in subsequent humidity cycles if 80% RH is not exceeded.

Khennouf et al. used Digital Image Correlation method to investigate the strain experienced by a textile [6]. The results, for both the textile and also for a historic tapestry investigated in situ in a historic house, showed that it is possible to quantify the global strain across a discrete area of an investigated object so that strain maps can be created to depict areas of high and low strain. The study also demonstrated the linear relationship between RH and strain in the RH mid-range; even small variations in RH produced positive to negative strain cycling. The creep strain experienced by a textile when a fixed load is applied over a long period of time was also investigated.

The analysed response pattern of historic textiles to RH variations gives rise to two potential damage mechanisms: stress building due to shrinkage of a textile restrained in its dimensional response, and the fretting fatigue when yarns move with friction against one another on cyclic extension and contraction. The latter process may be exacerbated by the self-loading of large, heavy, hanging textiles like tapestries. In order to assess rationally the threats posed to textiles by climate instability, the relationships between RH, moisture content and dimensional change were investigated in this study for a selection of fragments of historic silk and wool textiles dated to between the fifteenth and twentieth century. The hygral expansion results were compared with critical extensions obtained in tensile tests. Furthermore, the impact of a large number of extension cycles on textile performance was assessed.

Materials and methods [heading]

Several samples of historic textiles made of wool and silk were used in the testing programme. Two modern artist canvases were also investigated. Details of the textiles are given in Table 1.

Water vapour adsorption and desorption isotherms were determined at 24 ^{o}C and for an RH range between 0 and 80%. The measurements were done gravimetrically with the use of a vacuum microbalance from CI Electronics Ltd (Salisbury, UK). Typically, a piece of textile (0.05-0.1 g) was weighed and outgassed prior to a measurement under a vacuum of a residual pressure less than 0.1 Pa. The aim was to move air out of the textile and to eliminate most of the species physisorbed during the storage of the sample, especially adsorbed water. A vacuum was maintained until a constant weight was obtained, then subsequent quantities of water vapour were introduced, and the respective mass increases due to the sorption and the equilibrium pressures were finally recorded. The equilibrium moisture content (EMC) values were calculated on the basis of the initial weight of the outgassed sample. The process was fully automated and rapid; the measuring of 10 adsorption and 10 desorption points took on average 15 hours.

The tensile properties were determined using a Universal Testing Machine (UTM) from Hegewald & Peschke MPT GMBH (Nossen, Germany) for textile specimens 80-100 mm long and 50 mm wide. All measurements were taken under laboratory conditions at RH values ranging between 30 and 50% and at temperatures ranging between 22 and 24 ^{o}C. The rate of tension loading was between 1 and 2 mm/min. For some specimens, additional tests were carried out at a low loading rate of 0.003 mm/min to measure the effect of creep.

Using the UTM, cycles of strain were produced by mechanical stretching of the specimens with an amplitude of 1%, that is, exceeding the maximum dimensional changes of unrestrained textiles induced by fluctuations of RH as determined in the hygral expansion measurements. After each cycle, the position of zero strain was re-initialized to compensate for incomplete strain recovery when the stress was removed. The frequency of the strain cycles was approximately 0.3 Hz, which was low enough to prevent the specimen from heating. The specimens were subjected to up to 100 000 cycles. The tensile properties of each tested sample were determined after the cycling to assess the possible impact of the fretting process. All the experiments were conducted at ambient RH ranging from 30 to 50% and at room temperature.

The dimensional change of textiles accompanying water vapour adsorption and desorption was measured using strips 80 x 20 mm^2. The measurements were taken in a specially built sample holder placed in a vacuum vessel connected to the same outgassing and water vapour dosing system used to determine the water vapour sorption isotherms; in fact the two measurements were taken simultaneously. The specimen was vertically oriented in the holder and its upper end was firmly stabilised. The lower end was free to move in the vertical direction and changes of its position were measured with 2 μm accuracy using an inductive transducer from RDP Electronics Ltd (Wolverhampton, UK). The specimen was loaded with force of 0.8 N (40 N/m) sufficient to keep it in a vertical plane. Both expansion and shrinkage branches of the dimensional change isotherm were recorded.

On-site monitoring of the dimensional response of a historic textile [heading]

Fibre Bragg grating sensors were applied to measure strains in a seventeenth century Flemish wool tapestry from the collection of the National Museum in Krakow exhibited in the Gallery of Decorative Art (Figure 1). The sensor, the data acquisition system and the method of strain calculation were described in detail in Ref. [7]. A sensor fibre head was attached to the textile by magnetic clamps to record, at one minute intervals, the strain generated along the vertical direction in the upper parts of the textiles, where stresses are the largest. Temperature-induced expansion and contraction recorded by a second, reference, Bragg grating sensor which was not attached to the textile, allowed temperature correction of the strain values measured on the textile. Ambient temperature and RH were also measured using a radio monitoring system from IMC Group Ltd (Letchworth, Hertfordshire, UK).

Results and discussion [heading]

Sorption isotherms [sub-heading]

By way of example, the adsorption and desorption isotherms for one wool and one silk specimen investigated are shown in Figure 2. Hysteresis loops appear between the adsorption and desorption branches; these show the higher moisture content during desorption when compared to that during adsorption at any given RH value. This phenomenon is associated with the swelling of a non-rigid textile structure in the course of adsorption, so that the effect is in fact a manifestation of elastic hysteresis [8].

The three-parameter Guggenheim-Andersen-de Boer (GAB) sorption equation was used to interpret the sorption data for textile materials by expressing the equilibrium moisture content as a function of RH [9]:

$$EMC(RH, T = const.) = \frac{V_m * c * k * RH/100}{(1 - k * RH/100)(1 + (c-1)k * RH/100)} \quad (1)$$

where EMC is the equilibrium moisture content in per cent of dry material, RH - relative humidity in per cent, V_m - the monolayer capacity in the same units as EMC, c – an energy constant related to the difference of free enthalpy (standard chemical potential) of water molecules in the upper sorption layers and in the monolayer, and k - the third parameter, related in turn to the difference of free enthalpy of water molecules in the pure liquid and the upper sorption layers.

The GAB constants V_m, c and k were determined by a least-squares regression of the adsorption data in the range 5%<RH<80%. The curves calculated using the GAB sorption equation are compared in Figure 2 with the experimental data**.** The sets of values of the GAB constants obtained from the regression of the experimental data for all 13 textiles analysed are summarized in Table 1 for the adsorption. It should be stressed at this point that, because of the hysteresis loop, the adsorption branch only yields meaningful physical parameters - the monolayer capacity and the energy constant.

Tensile properties [sub-heading]

Textiles are deformed by an applied force and the load-extension curves illustrate subsequent phases of deformation when the material is subjected to an increasing load (Figure 3). It is worthwhile to note that load is expressed as the force per width of a specimen since it is impractical to determine the cross-sectional area of a textile and thus to calculate the stress.

It is generally accepted that the initial part of the load-extension curve corresponds to a slack region, before the tension is taken up by the textile, followed by a crimp-removal region. Only the post-initial relationship reflects stretching of the yarns (the Hookean region). A very low stiffness of approximately1.8 kN/m calculated using the slope of the initial linear part of the load-extension curve for the weft direction in rug 1 (Figure 3B) indicates that the 0-1.4% extension range corresponds to the removing of slack and the pulling-out of the crimp. Above an extension of approximately 5%, a transition to the Hookean region manifests as a gradual increase in the stiffness. The load-extension relationship becomes finally linear in the extension range 12.5-16.5% (load range between 2.5 and 5.5 kN/m). In the study of fabrics for artist's canvas [5], the stiffness in the stretched yarns (Hookean region) was measured at a load of 2 kN/m whereas the high-load linear part of the load-extension curve for a wool fabric representing a historical tapestry was 2 – 4 kN/m [6]. The high-load stiffness for the rug investigated in this study was 106 kN/m. Beyond an extension of 16.5% the load-extension curve begins to deviate significantly from a straight line, which is known to define the upper limit of the elastic range at which non-recoverable deformation begins. The final part of the curve shows a progressive drop in load values corresponding to a successive yarn fracture. Due to the manufacturing method, the perpendicular weave directions, weft and warp, show different load-extension behaviour. The weft direction in the rug investigated is more flexible than the warp. Also the extension at failure in the weft direction is 20% compared to 15% in the warp. Reduced stiffness and a larger value of the critical extension in the weft direction are an outcome of the less ordered twist in the weft yarns when compared to the warp yarns.

The load-extension behaviour in terms of the critical extension and failure mechanism is a characteristic feature of every historic textile. The load-extension curve for the weft direction in a densely woven silk damask demonstrates a very limited crimp-removal region, high stiffness in the stretched yarns (770 kN/m) and the onset of failure at extension of only approximately 1% (Figure 3C). The tensile parameters of the textiles investigated in this study are presented in Table 2. It should be noted that extension and load at failure in the table are defined as the values at which non-recoverable deformation of a textile begins. The selection is rather conservative as the textile must be stretched considerably beyond the critical extension thus defined before the material fails via yarn fracture.

Additional information on the subsequent stages of the textile deformation is provided by comparing load-extension curves obtained at rates of loading varying significantly between 200 and 0.003 mm/min (Figure 4). Stretched yarns experience time-dependent behaviour – they creep when there is a fixed load applied and relieve stress when a fixed extension is applied. The load-extension relationships obtained at loading rates of 200 and 2 mm/min differ little and illustrate the initial or short-term extension values at increasing loading with a minimal creep/relaxation component due to the short duration of the load application. Creep/relaxation manifests as an increasing decrease in stiffness for the slow loading at 0.003 mm/min, though the effect is limited until an extension of approximately 3%. The observation confirms that the removal of slack and the pulling-out of the crimp predominates in the 0-3% extension range (for unstretched yarns).

Moisture-related strain [sub-heading]

The tensile testing described in the preceding section ultimately took specimens to high force and extension levels that are not relevant to most textiles on display as such extensions would cause deformation and physical failure. A large tapestry monitored in this project, hanging vertically on the wall, can be considered the worst case in terms of the load experienced by a textile as a result of carrying its own weight. The tapestry was 2.6 m wide and 3.2 m high and had a mass of approximately 10 kg. The load experienced in the weft direction at the top of the tapestry was thus 38 N/m. The corresponding strain in the weft direction that can be determined from the early part of the load-extension curve is 0.76% which agrees well with strains recorded at such a loading for a wool fabric representing a historic tapestry [6], and in the warp direction of several modern linen fabrics [4].

Expansion produced by a rise in RH adds to the extension caused by loading. A general pattern of moisture-related dimensional change for textiles investigated in this study was evident, though the detailed characteristics of the response differed. The dimensional response of the wool fabric loaded with 40 N/m and subjected to an RH cycle between a dry condition and 80% RH is shown in Figure 5. There is a significant difference in the moisture-related dimensional change between the weft and warp directions. The specimen expands in the weft direction in the entire RH range investigated whereas no moisture-related response is observed in the warp. A small irreversible elongation of 0.1% is observed in the weft direction after the first moisture adsorption-desorption cycle whilst the second expansion-shrinkage cycle is fully reversible. As the ultimate (equilibrium) strain at a given RH is obviously dependent on the EMC in the material, a convenient way of expressing the expansion and shrinkage behaviour of a textile is to plot strain as a function of EMC rather than RH (Figure 6).

The relationship between the dimensional change and EMC is close to linear up to approximately 6% EMC which corresponds to about 30% RH. Then a gradual downward deviation from the initial linear plot is observed, pointing to an onset of forces exerted by expanded yarns upon each other and restraining the free expansion of the textile. These forces, however, do not lead to shrinkage even at the upper limit of the RH range selected. Reducing the RH to a dry condition reversed the textile's elongation. A hysteresis loop between the adsorption and desorption branches is observed, that is higher moisture-related strain during desorption when compared to that during adsorption at any given EMC value. This phenomenon can be generally associated with changes in weave geometry brought about by the fibre swelling. The initial stiffness of the textile (the early part of a load-expansion curve) is enhanced by rising RH due to such changes [1,11]. One can, therefore, speculate that only when the textile becomes dry and flexible can the structural alteration engendered at high RH be fully reversed.

The irreversible elongation in the low-load range can be very considerable as observed for a tapestry (tapestry 1) with thick wool weft yarns of loose twist and a high degree of crimp (Figure 7). Moreover, the observation indicates a stepwise accumulation of the irreversible yarn elongation over subsequent moisture-induced expansion/shrinkage cycles, though the magnitude of the irreversible change gradually decreases with each cycle.

The reversible strain-EMC plot in Figure 7 is again approximately linear up to approximately 6% EMC, then a strong gradual downward deviation is observed, pointing to a shrinkage above 9% EMC or 50% RH. A significant hysteresis loop between the adsorption and desorption branches is observed. The strain-EMC plots in the responsive weft direction - for the sake of clarity, the adsorption branches only - recorded in the final RH cycle with minimal irreversible elongation are shown in Figure 8 for all the wool textiles investigated.

The red silk satin also shows a considerable irreversible elongation in the weft direction (Figure 9). However, in contrast to wool textiles with loosely twisted yarns, the strain-EMC plots in Figure 9 do not show any downward deviation at high RH range. The textile expands up to approximately 5% EMC at which RH level the dimensional change attains a plateau.

This points to a restraint in any further alteration in the weave geometry brought about by fibre swelling. The silk textile also differs from wool in the absence of any pronounced hysteresis loop between the expansion and shrinkage branches. As in the wool textiles investigated, the specimen shows insignificant moisture-related response in the warp direction.

The adsorption branches of the strain-EMC plots in the responsive weft direction - recorded in the final RH cycle with minimal irreversible elongation - for all the silk textiles investigated are shown in Figure 10.

The linen canvas 520 was an unusual textile, as it showed almost no moisture-related expansion in the initial 0-4% EMC or 0-30% RH region but beyond this a dramatic shrinkage of 1.2% was observed (Figure 11). An irreversible elongation of 0.1% occurred after the first moisture adsorption-desorption cycle whilst the second shrinkage cycle was fully reversible. Hedley (1988) observed similar irreversible dimensional changes in linen canvases which he explained as a plastic behaviour.

The adsorption branches of the strain-EMC plots in the warp direction for the two canvases – the linen canvas 520 and the cotton canvas investigated - are shown in Figure 12. The latter textile does not show any shrinkage force at a high RH range because its yarns are quite straight and have little crimp.

The moisture response plots make it possible to derive the cyclic dimensional changes which the textiles experience in their display environments in response to RH fluctuations. One wool and one silk textile (rug 2 and green damask) which showed the highest moisture-related dimensional response were selected for the calculations as these represented the worst cases of the study in terms of the susceptibility of the textile to humidity cycles (Figure 13). When the textiles experience RH variations between 25 and 75% RH, corresponding to RH variations of the highest amplitude recorded during a year in the display environment of the textile monitored in this study (see below), the dimensional response is 0.45% and 0.4% for wool and silk respectively.

Moisture-related strains of the Flemish tapestry in its display environment [sub-heading]

The on-site monitoring of strains generated by RH variations was carried out during one year for a Flemish wool tapestry from the collection of the National Museum in Krakow hung from the weft yarns as described above (Figure 14). The analysis of the recorded data indicated a significantly non-linear relationship between strain and RH (Figure 15).

The response followed the general pattern established in this work for the wool textiles (Figures 5-8): an initial expansion with increasing RH followed by shrinkage at high RH, with a hysteresis loop between the adsorption and desorption branches. The overall recorded expansion of the reference object was only around 0.05% during the year, an order of magnitude less than the worst-case moisture responses derived above.

Fatigue deterioration [sub-heading]

The load-extension curves for tapestry 2 in the weft direction subjected to strain cycles with an amplitude of 1%, simulating maximum dimensional changes of unrestrained textiles induced by RH fluctuations, are shown in Figure 16. The loads applied remained below 0.1 kN/m which is a typical load range experienced by textiles in realistic conditions of display. For example, the Flemish tapestry monitored in this project, hanging vertically, experienced a load of 0.04 kN/m as a result of carrying its own weight whereas Young and Hibberd [10] estimated that a load of 0.12-0.2 kN/m needs to be applied to a canvas to produce a tautness equivalent to a newly stretched painting. The initial loading cycles removed slack and pulled out the crimp producing an initial extension of 2.5% as analysed in detail above (Figure 3).

The textile structure stabilised after approximately 100 cycles (Figure 17) and further load-extension cycles were fully reversible i.e. the textile returned to its original shape when the applied stress was removed. The shape of the load-extension curves is in close agreement with the experimental work of Young et al. on the uniaxial properties of a variety of fabrics: non-linear shape in the 0 – 0.08 kN/m loading region and hysteresis on unloading associated with the presence of the frictional forces at the yarn cross-over points [5,10].

The results of cyclic loading illustrated in Figure 16 did not reveal the mechanical deterioration of the textile caused by a hypothetical accumulation of damage at the micro level commonly related to the fretting process. The load-extension curves for several original textile specimens and a specimen of the same textile subjected to a large number of stretching cycles (100 000 cycles for tapestry 1 and rug 1, all other samples 41 000 cycles) are within the natural variation of the textile mechanical behaviour (Figure 18). Tensile load and expansion at failure for the textiles before and after cyclic loading are compared in Table 2 and show close agreement. The observation is particularly illuminating for two silk textiles (brown taffeta and green damask) which exhibited low expansion at failure, of around 1%, comparable with the amplitude of the stretching cycles of the fatigue testing.

Additional cycling tests were carried out on a tapestry specimen containing weft yarns of various colours joined with slit stitching. This experiment was carried out to check how a large number of cycles affects areas of stress accumulation. Similarly to the homogeneous samples, the results showed no significant change in either the reversibility of the loading-extension cycles or the mechanical properties. This confirmed that the historical samples were not significantly affected by thousands of cycles.

Conclusions [heading]

The dimensional response of a range of textiles to changes in RH, and the critical levels of strain at which the materials begin to fail physically, were systematically examined, providing insight into potential textile damage mechanisms: stress building due to shrinkage of a textile restrained in its dimensional response, and the fretting fatigue when friction causes yarns to move against each other on cyclic extension and contraction. It was assumed that the historic textiles would have undergone irreversible loading cycles in the past. This study aimed to assess whether museum display conditions contributed accumulating irreversible deformation reflecting deterioration of yarns caused by fatigue.

Decreasing RH produces shrinkage in a textile which induces tensile stress when the textile is restrained in its dimensional response. The restraint may result from fixing the textile in a rigid construction which restricts movement, in upholstered furniture or in frames to decorate walls, or by supporting a historic textile with another textile which responds differently to RH changes. The investigations carried out in this study indicate that if a wool textile which is highly responsive to moisture is lightly stretched and equilibrated at an average RH of 50% in its display environment, then even the fall of the parameter in winter to a very low level of 10% will reduce the moisture content of the wool from 11 to 4% and produce a shrinkage of 0.6%. For a silk textile which is highly responsive to moisture, the same RH fall would produce a moisture content drop from 5.5% to 2% and a shrinkage of 0.35%. The calculated dimensional changes are insignificant in terms of failure risk unless the textile was initially excessively strained in its mounting.

The risk of climate-induced fretting fatigue was assessed, assuming reasonably that the expansion and shrinkage cycles induced by RH variations can be simulated by cyclic mechanical stretching of a textile. Even in the worst case scenario when diurnal RH variations in a museum are as pronounced as to produce a strain of 1% for a wool tapestry, 274 years of object storage in such conditions would not cause significant damage due to fretting fatigue.

The established relationships between RH, moisture content and dimensional change also allow the self-loading of large hanging textiles like tapestries to be assessed rationally. The load experienced in the weft direction at the top end of a large tapestry, monitored in this project, was 38 N/m as a result of carrying its own weight. For a yearly RH variation ranging from 25% in winter to 75% in summer, the gain in textile mass and the resulting load is 7% i.e. 2.7 N/m. The increased load produces an insignificant increase in strain of the order of 0.02% which is still far from the critical strain at which the textile fails physically. Therefore the textiles sustain increases in weight due to sorption of moisture without damage unless they are so degraded that the extension produced by self-loading is close to the critical level.

ACKNOWLEDGEMENTS

This research was supported by a grant from Iceland. Lichtenstein and Norway through the European Economic Area (EEA) Financial Mechanism within the research project *Direct monitoring of strain for protection of historic textiles and paintings on canvas* implemented in 2008–2011.

REFERENCES

1. Ballard, M. (1997) More on moisture: cohesive, temporary, or permanent set and hygral expansion. *Textile Conservation Newsletter* **32**, 5-20.
2. Hedley, G. (1988) Relative humidity and the stress/strain response of canvas paintings: uniaxial measurements of naturally aged samples. *Studies in Conservation* **33**, 133-48.
3. Mecklenburg, M.F. (2007) *Determining the Acceptable Ranges of Relative Humidity and Temperature in Museums and Galleries. Part 1, Structural Response to Relative Humidity*. Washington: Museum Conservation Institute, The Smithsonian Institution, Washington [accessed 4 April 2014]. Available at: http://si-pddr.si.edu/handle/10088/7056
4. Krarup Andersen, C. (2013) *Lined Canvas Paintings.* PhD Thesis, Royal Academy of Fine Arts, Schools for Architecture, Design and Conservation, Copenhagen.
5. Young, Ch. and Jardine, S. (2012) Fabrics for the twenty-first century: as artist canvas and for the structural reinforcement of easel paintings on canvas. *Studies in Conservation* **57**, 237-53.

6. Khennouf, D., Dulieu-Barton, J.M., Chambers A.R., Lennard, F.J. and Eastop, D.D. (2010) Assessing the feasibility of monitoring strain in historical tapestries using digital image correlation. *Strain* **46**, 19-42.
7. Zawadzki, W., Bartosik, M., Dzierżęga, K., Bratasz, Ł., Łukomski, M. and Peacock, E. (2012) Application of fibre Bragg gratings for strain measurement in historic textiles and paintings on canvas. *Optica Applicata* **XLII**, 503-517.
8. Sing, K.S.W., Everett, D.H., Haul, R.A.W., Moscou, L., Pierotti, R.A., Rouquerol, J. and Siemieniewska, T. (1985) Reporting physisorption data for gas solid systems with special reference to the determination of surface area and porosity. *Pure Appl. Chem.* **57**, 603-619.
9. Timmermann, E.O. (2003) Multilayer sorption parameters: BET or GAB values? *Colloids and Surf. A: Physicochem. Eng. Aspects* **220**, 235-260.
10. Young, Ch.R.T. and Hibberd, R.D. (1999) Biaxial testing of paintings on canvas. *Studies in Conservation* **44**, 129-141.
11. Mecklenburg, M.F (2005) The structure of canvas supported paintings, In: *Preprints of the International Conference on Painting Conservation. Canvases: Behavior, Deterioration and Treatment* (V. Guerola Blay, M. Castell Augusti, S. Martin Rey and L. Fuster López, Eds) Universitat Politècnica de València, Valencia, 119-155.

LEGEND OF FIGURES

1. A seventeenth-century Flemish tapestry for which on-site monitoring of the dimensional response was carried out
2. Adsorption and desorption isotherms of water vapour for historic wool and silk textiles (checked wool fabric and red satin): the black lines are from the regression of the experimental data using the GAB equation for the adsorption branch
3. The load-extension curves for textiles subjected to tension: (A) rug 1; (B) the initial part of the curves for rug 1; (C) green damask
4. The effect of rates of loading on the load-extension relationships for rug 1 in the weft direction
5. Moisture-related strain of the checked wool fabric plotted as a function of RH
6. Moisture-related strain of the checked wool fabric in the weft direction plotted as a function of the equilibrium moisture content
7. Moisture-related strain of tapestry 1 in the weft direction plotted as a function of the equilibrium moisture content
8. Adsorption branches of the moisture-related strain of the wool textiles in the weft direction, recorded in the final RH cycle, plotted as a function of the equilibrium moisture content
9. Moisture-related strain of red satin plotted as a function of the equilibrium moisture content
10. Adsorption branches of the moisture-related strain of the silk textiles in the weft direction, recorded in the final RH cycle, plotted as a function of the equilibrium moisture content
11. Moisture-related strain of the linen canvas 520 in the warp direction plotted as a function of the equilibrium moisture content
12. Adsorption branches of the moisture-related strain in the canvases in the warp direction, recorded in the final RH cycle, plotted as a function of the equilibrium moisture content
13. Moisture-related strain of wool rug 2 and green silk damask in the weft direction, plotted as a function of RH. Dimensional responses for RH variations between 25 and 75% are marked
14. RH and strain along the weft yarns of the Flemish tapestry monitored over one year
15. The relationship between strain along the wool weft yarns of the Flemish tapestry and RH

16. Cyclic load-extension for tapestry 2 in the weft direction
17. Initial elongation of tapestry 2 in the weft direction as a function of a number of stretching cycles
18. The load-expansion curves for rug 1 before and after cyclic loading, consisting of subjecting the specimen to 41 000 stretching cycles

A seventeenth-century Flemish tapestry for which on-site monitoring of the dimensional response was carried out
331x496mm (72 x 72 DPI)

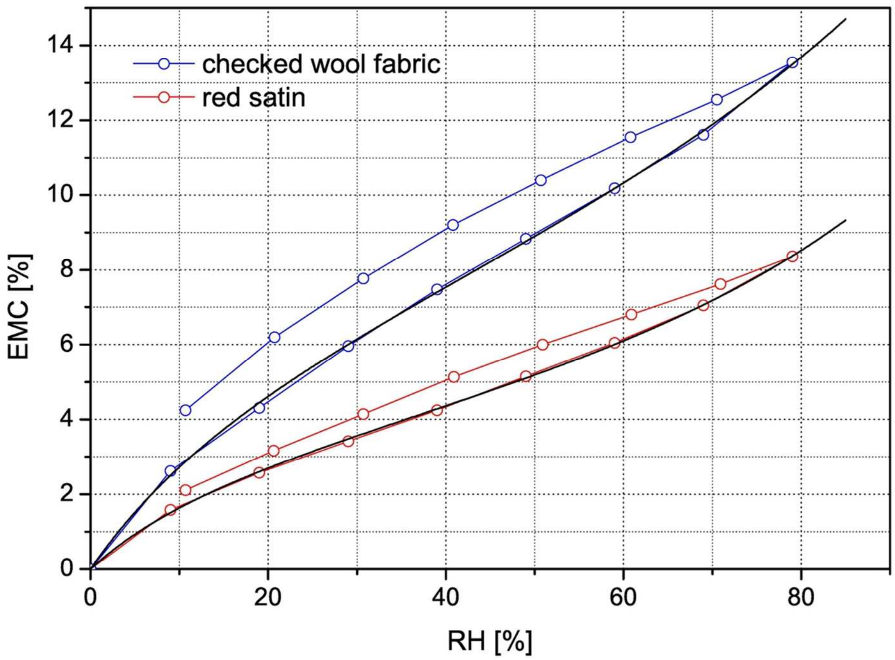

Adsorption and desorption isotherms of water vapour for historic wool and silk textiles (checked wool fabric and red satin): the black lines are from the regression of the experimental data using the GAB equation for the adsorption branch
112x79mm (300 x 300 DPI)

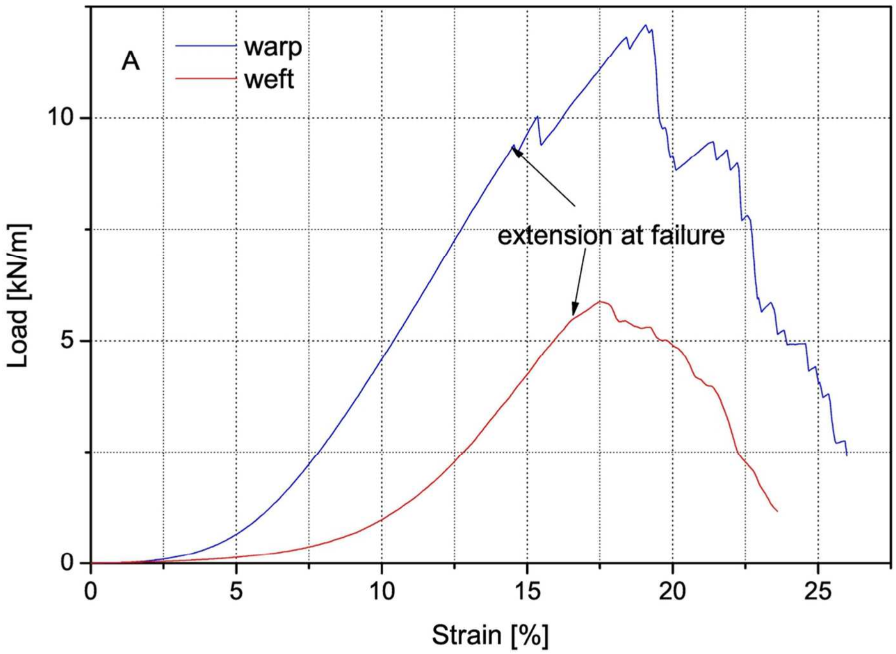

The load-extension curves for textiles subjected to tension: (A) rug 1; (B) the initial part of the curves for rug 1; (C) green damask
111x77mm (300 x 300 DPI)

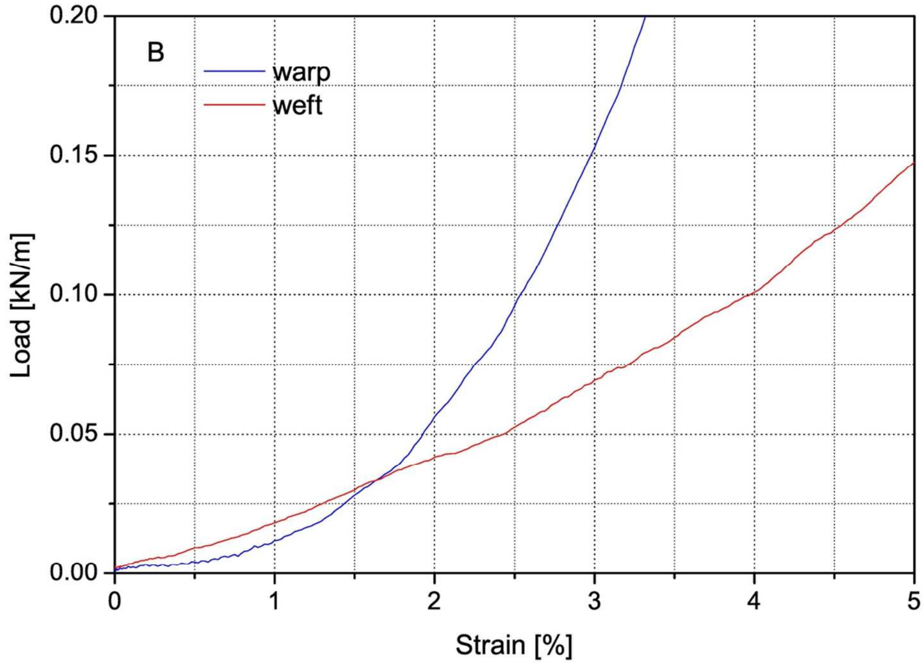

as above
111x77mm (300 x 300 DPI)

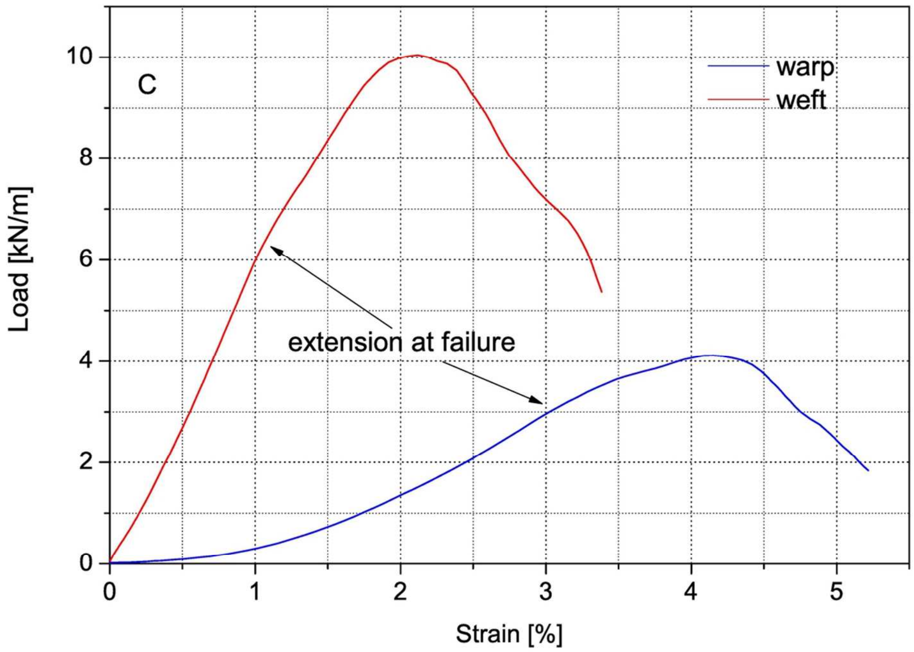

as above
111x77mm (300 x 300 DPI)

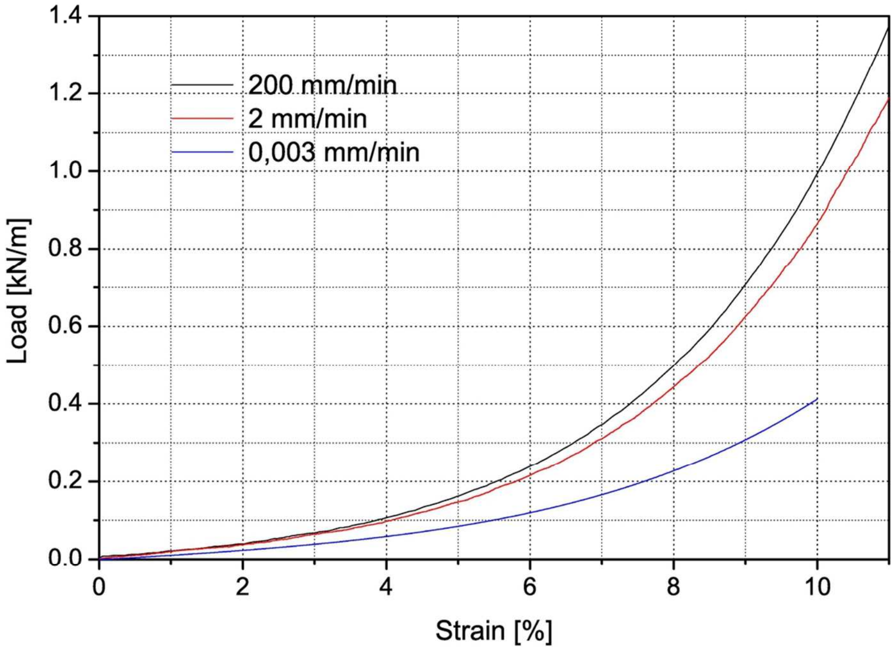

The effect of rates of loading on the load-extension relationships for rug 1 in the weft direction
111x77mm (300 x 300 DPI)

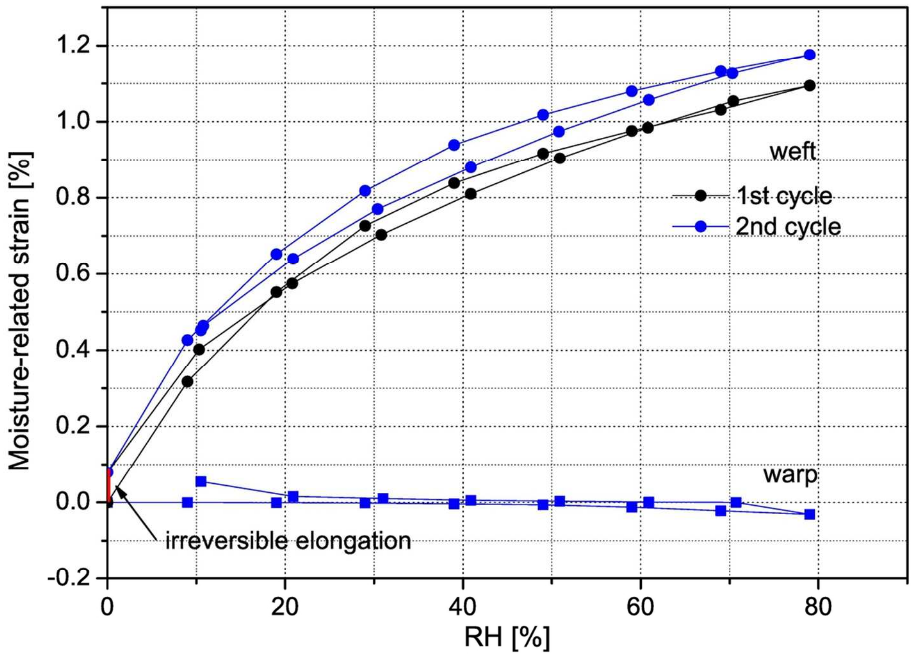

Moisture-related strain of the checked wool fabric plotted as a function of RH
114x82mm (300 x 300 DPI)

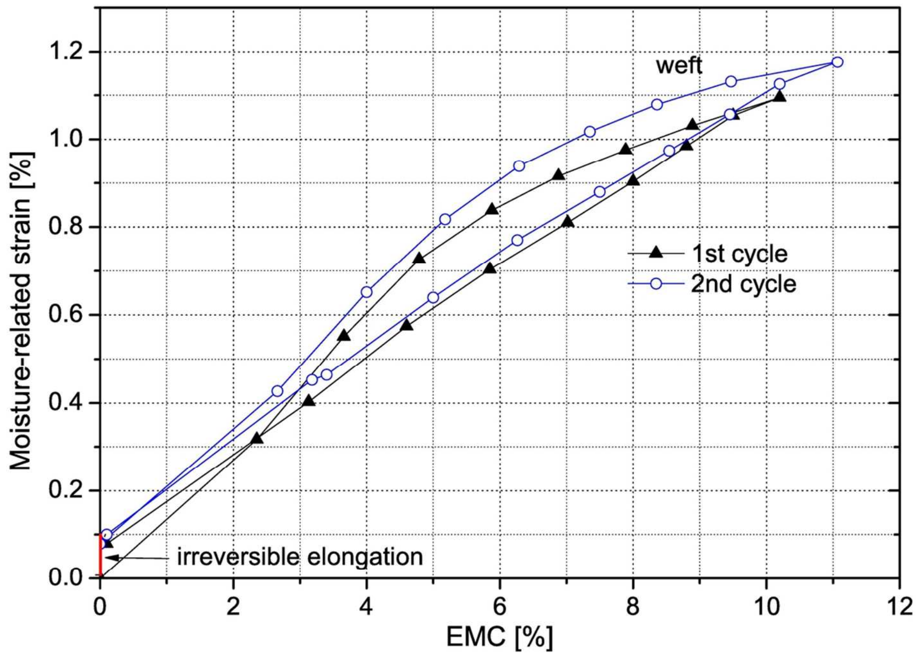

Moisture-related strain of the checked wool fabric in the weft direction plotted as a function of the equilibrium moisture content
114x82mm (300 x 300 DPI)

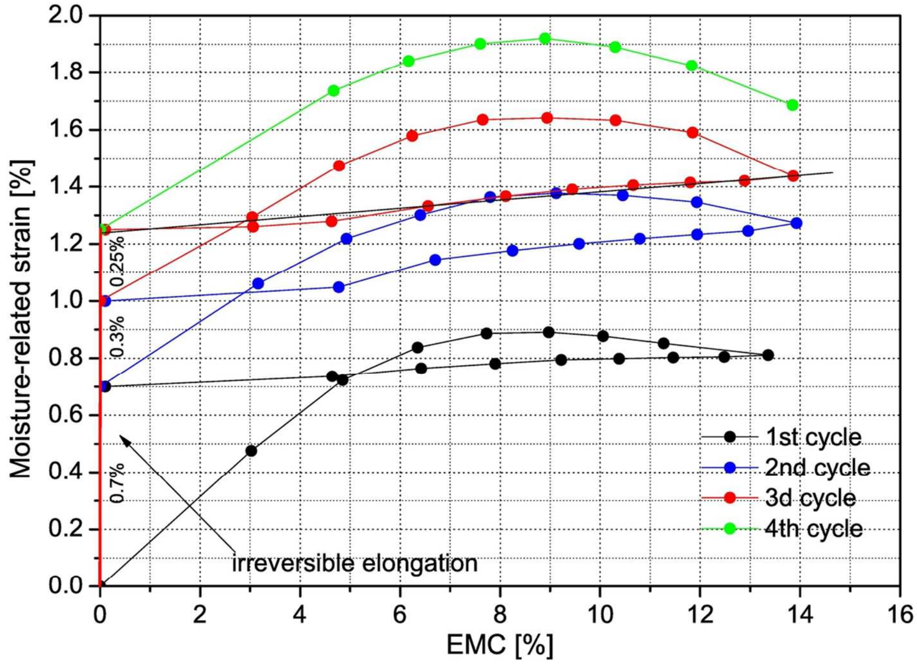

Moisture-related strain of tapestry 1 in the weft direction plotted as a function of the equilibrium moisture content
114x82mm (300 x 300 DPI)

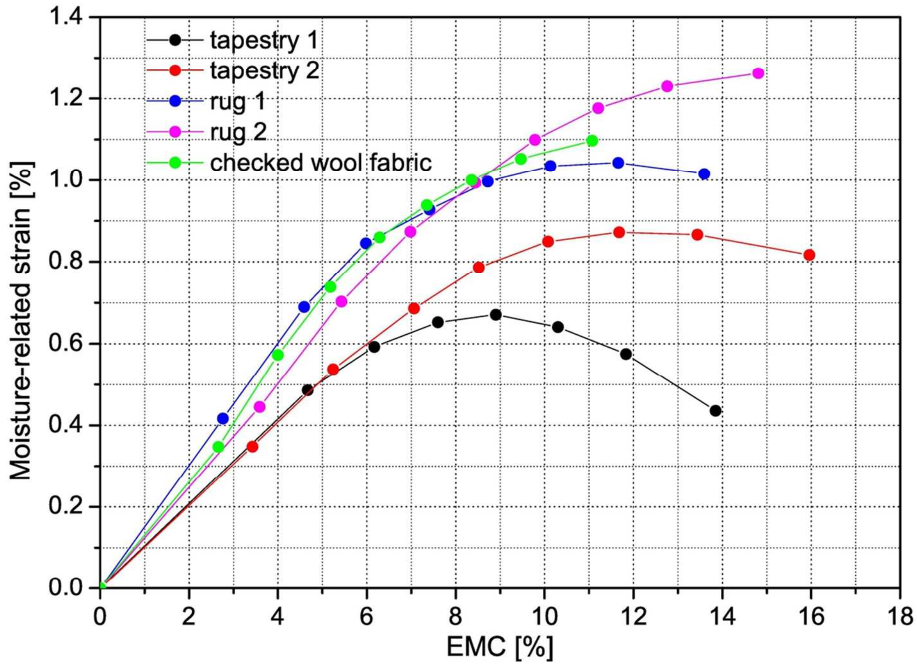

Adsorption branches of the moisture-related strain of the wool textiles in the weft direction, recorded in the final RH cycle, plotted as a function of the equilibrium moisture content
114x82mm (300 x 300 DPI)

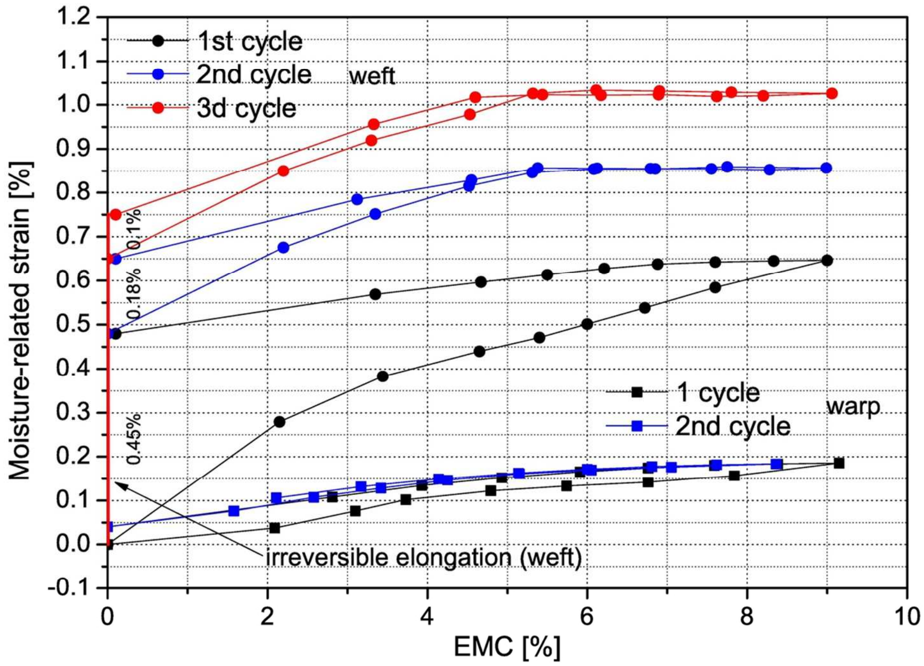

Moisture-related strain of red satin plotted as a function of the equilibrium moisture content
114x82mm (300 x 300 DPI)

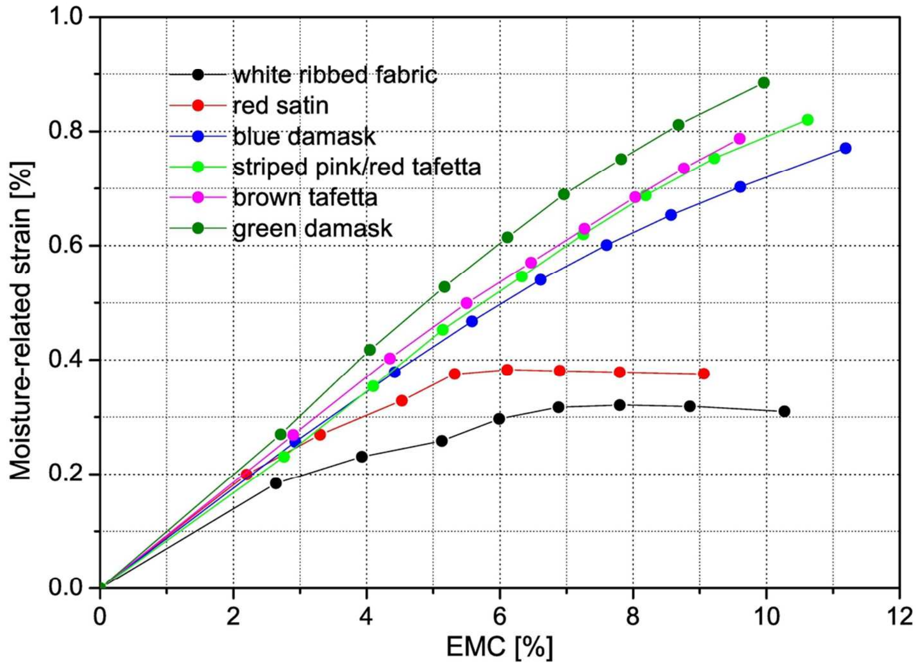

Adsorption branches of the moisture-related strain of the silk textiles in the weft direction, recorded in the final RH cycle, plotted as a function of the equilibrium moisture content
114x82mm (300 x 300 DPI)

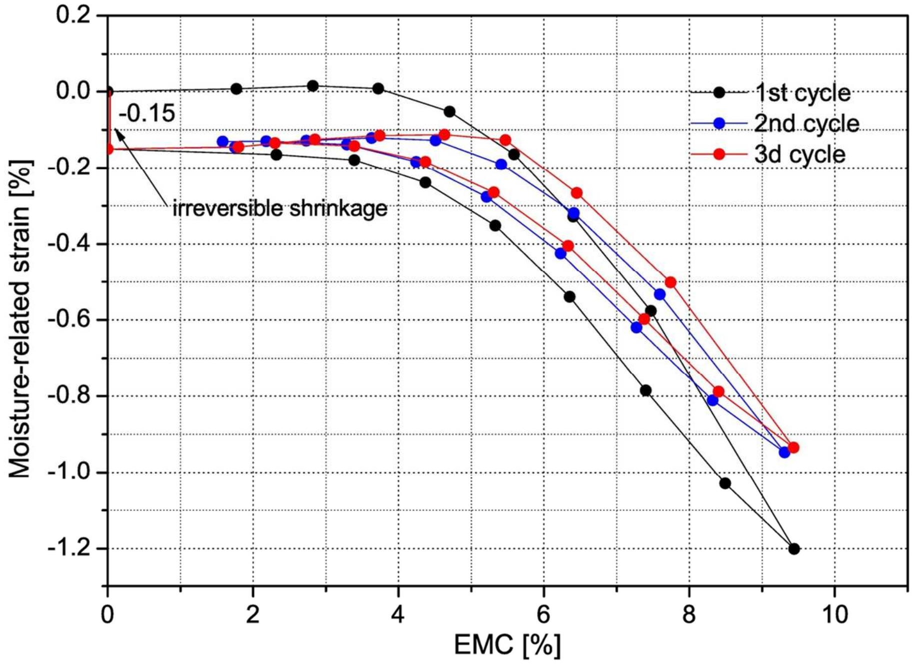

Moisture-related strain of the linen canvas 520 in the warp direction plotted as a function of the equilibrium moisture content
114x82mm (300 x 300 DPI)

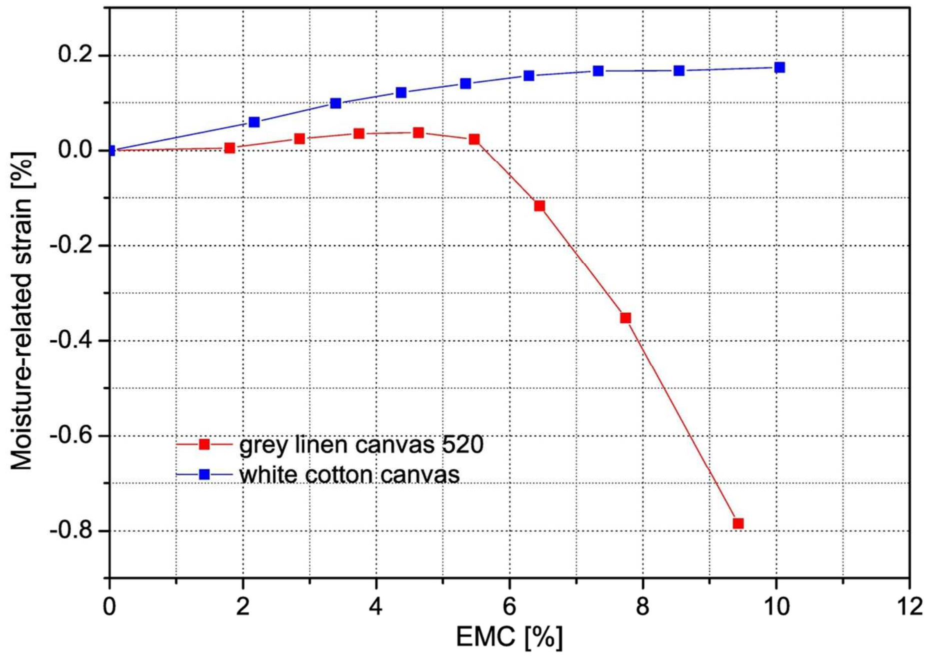

Adsorption branches of the moisture-related strain in the canvases in the warp direction, recorded in the final RH cycle, plotted as a function of the equilibrium moisture content
114x82mm (300 x 300 DPI)

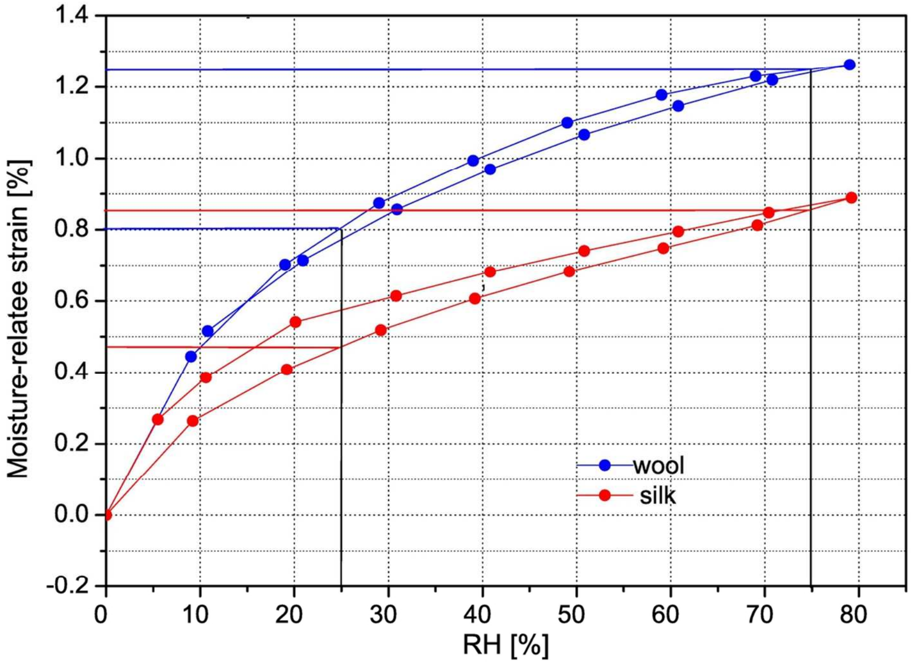

Moisture-related strain of wool rug 2 and green silk damask in the weft direction, plotted as a function of RH. Dimensional responses for RH variations between 25 and 75% are marked
114x82mm (300 x 300 DPI)

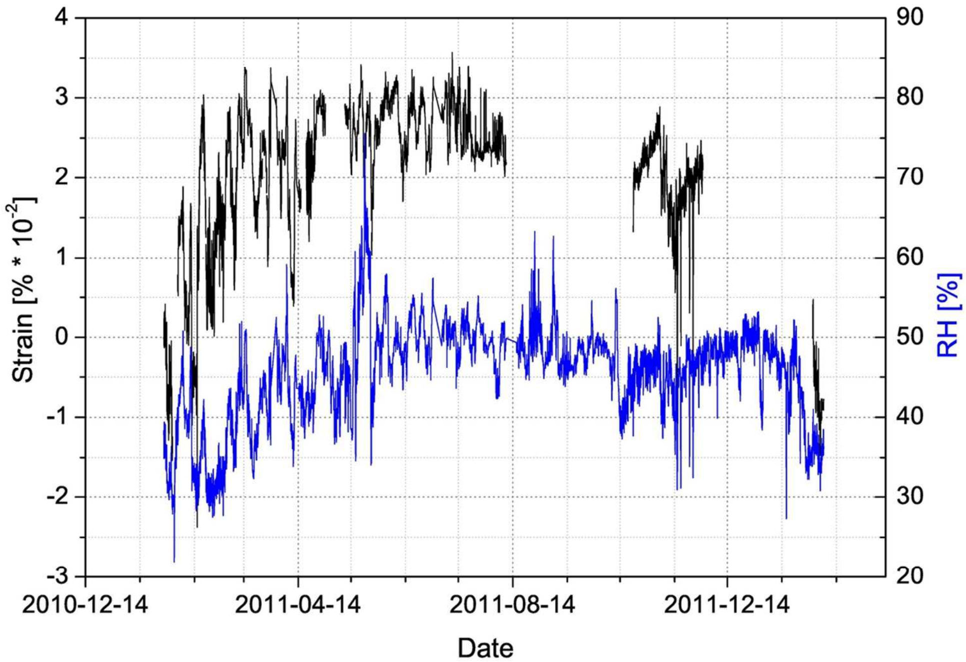

RH and strain along the weft yarns of the Flemish tapestry monitored over one year
112x78mm (300 x 300 DPI)

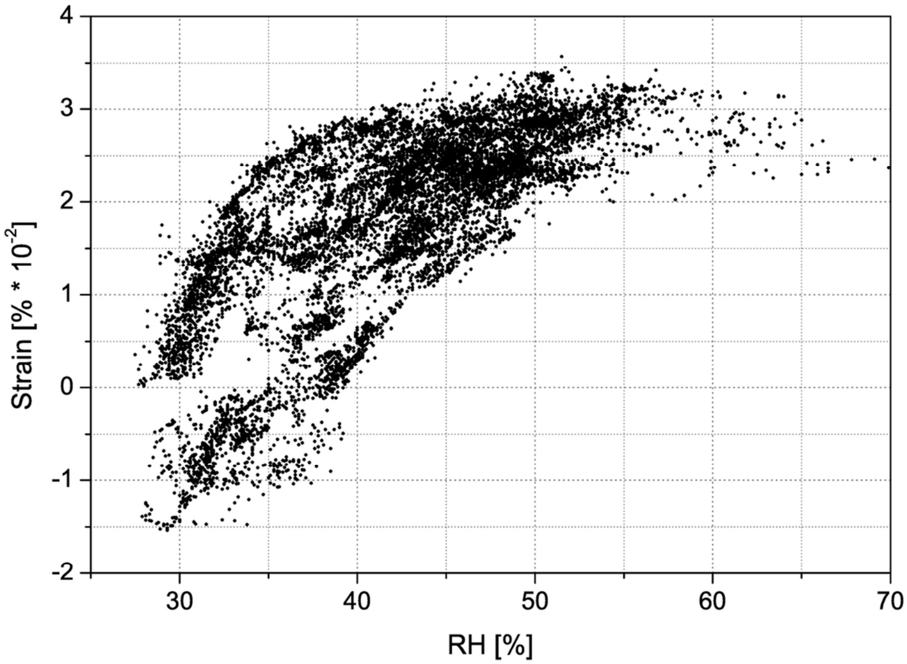

The relationship between strain along the wool weft yarns of the Flemish tapestry and RH
111x77mm (300 x 300 DPI)

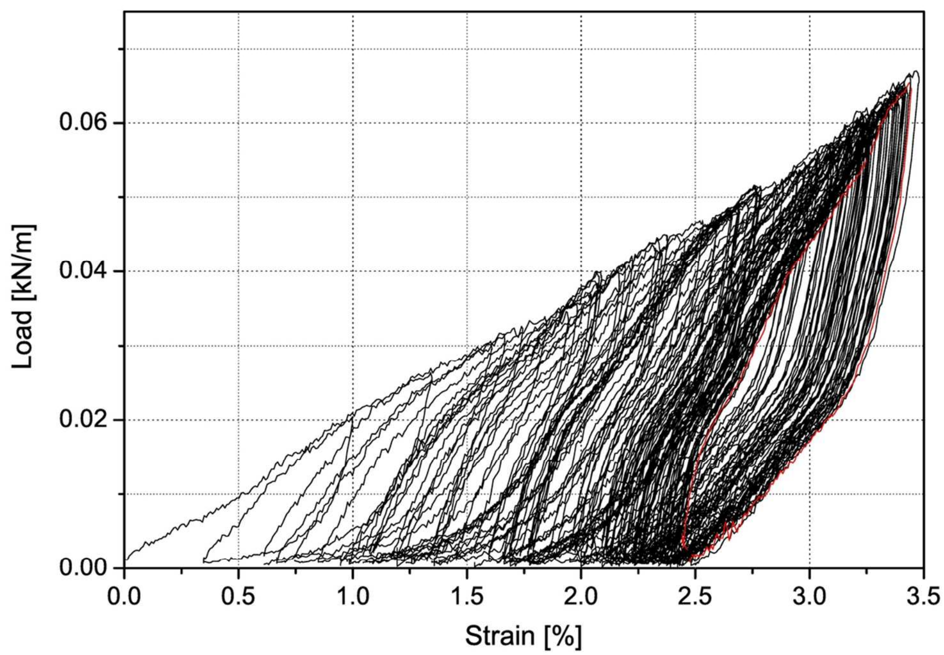

Cyclic load-extension for tapestry 2 in the weft direction
111x77mm (300 x 300 DPI)

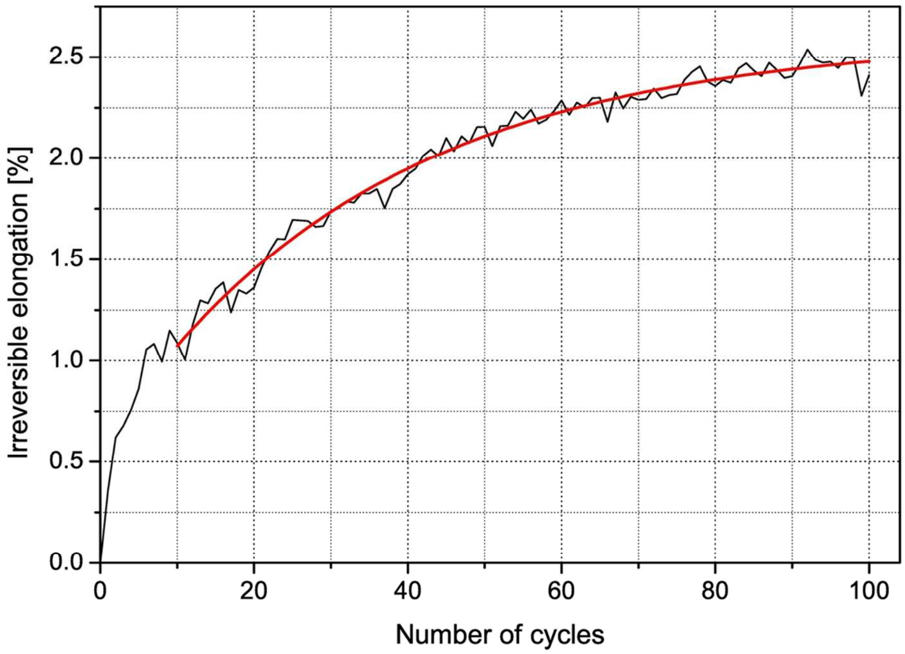

Initial elongation of tapestry 2 in the weft direction as a function of a number of stretching cycles
111x77mm (300 x 300 DPI)

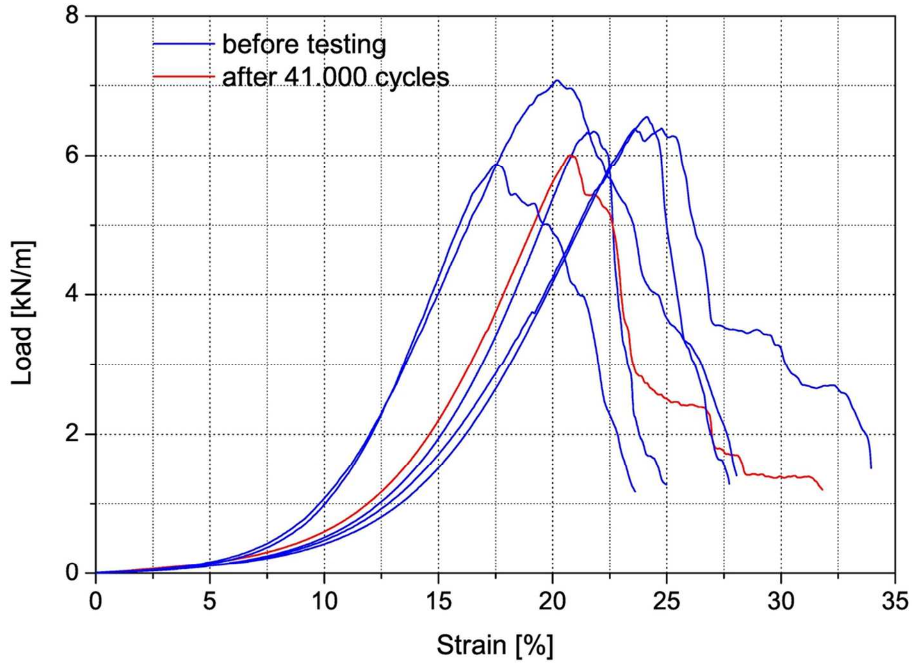

The load-expansion curves for rug 1 before and after cyclic loading, consisting of subjecting the specimen to 41 000 stretching cycles
111x77mm (300 x 300 DPI)

Table 1. Textile details and water vapour sorption

Textile	Weave technique	Fibre material	Weave count yarns/cm	GAB parameters			Moisture content [%] at 80% RH
				V_m	c	k	
Tapestry 1, first half of the eighteenth century	tapestry weave	wool weft	20	8.58	10.3	0.632	15.7
		linen warp	6				
Tapestry 2, second half of the eighteenth century	tapestry weave	wool weft	18	8.07	9.74	0.625	15.8
		linen warp	4				
Rug 1, second half of the nineteenth century	weft-faced plain weave or Kilim weave	wool weft	9	7.66	12.5	0.659	15.6
		linen warp	3				
Rug 2, first half of the twentieth century	weft-faced plain weave or Kilim weave	wool weft	16	7.75	10.7	0.648	14.8
		linen warp	5				
Checked wool fabric, second half of the nineteenth century	plain weave 1/1	wool weft	14	6.07	11.1	0.590	11.1
		wool warp	15				
White ribbed silk	warp-faced ribbed	silk weft,	27	5.57	13.3	0.627	10.4

fabric, first half of the nineteenth century	plain weave	alternate thin and thick yarns					
		silk warp	52				
Red satin, second half of the eighteenth century	8-end satin weave, interruption 4	cotton weft	29	5.20	11.4	0.592	9.1
		silk warp	173				
Blue damask, second half of the fifteenth century	5-end satin weave, interruption 2	silk weft	22	6.13	13.7	0.618	11.2
		silk warp	80				
Striped pink/red tafetta, second half of the nineteenth century	plain weave 1/1	silk weft	48	5.98	12.4	0.609	10.6
		silk warp	80				
Green damask	5-end satin weave	silk weft	48	5.90	13.4	0.574	10.0
		silk warp	80				
Brown taffeta, with woven pattern	warp-faced ribbed plain	silk weft	22	7.11	14.8	0.436	9.6

	weave	silk warp	60				
	supplementary weft yarns float over warp yarns	silk weft	22				
Grey canvas 520	twill weave 2/1	linen weft	20	4.10	8.31	0.749	10.6
		linen warp	30				
White canvas	plain weave 1/1	cotton weft	14	4.73	7.45	0.703	9.6
		cotton warp	14				

Table 2. Tensile properties

Textile	Weft direction					Warp direction			
	Before cycles		After cycles		Stiffness [kN/m] (Hookean range) [%]	Before cycles		After cycles	
	Load at failure [kN/m]	Extension at failure [%]	Load at failure [kN/m]	Extension at failure [%]		Load at failure [kN/m]	Extension at failure [%]	Load at failure [kN/m]	Extension at failure [%]
Tapestry 1	6.3	12.8	4.8	12.0	77 (6.5;11.5)	10.2	3.8	10.6	3.0
Tapestry 2	5.0	25.0	4.7	23.0	57 (17.5;23)	13.0	10	8.0	9.0
Rug1	5.5	16.5	5.1	21.3	106 (12.5;16.5)	9.0	13.5	9.5	14.4
Rug2	11.3	18.8	10.4	22.5	95 (9.5;16)	2.7	13.7	1.3	12.7
Checked wool fabric	1.3	14.9	-	-	20	2.7	3.4	-	-

					(10.5;14.5)				
White ribbed silk fabric	1.4	12.7	1.1	9.0	12.5 (3.5;11.5)	6.5	3.3	4.6	3.2
Red satin	10.2	2.1	-	-	806 (1.5;2.1)	2.1	3.7	-	-
Blue damask	8.0	3.4	-	-	314 (1.5;2.6)	7.0	4.9	-	-
Striped pink/red tafetta	10.9	3.7	9.7	3.5	323 (0;2.5)	2.2	11.3	2.0	9.7
Brown taffeta	7.0	1.0	3.9	1.0	464 (0.7;1.0)	3.1	9.0	3.0	6.0
Green damask	6.5	1.1	6.3	1.1	769 (0.2;1.1)	3.3	3.0	2.4	3.0
Grey canvas 520	8.8	3.9	-	-	300 (1.5;3.8)	19.2	10.7	-	-
White canvas	15.9	18.4	15.8	18.4	189 (13.8;18.4)	11.2	9.0	11.3	9.0